

THE PHENOMENA OF ELECTORRHEOLOGICAL FLUID BEHAVIOR BETWEEN TWO BARRIERS UNDER ALTERNATIVE VOLTAGE

M. L. SZARY

Southern Illinois University Carbondale
College of Engineering
Department of Technology
Carbondale, Illinois 62901, USA
e-mail: szary@enr.siu.edu

(received 18 March 2004; accepted 2 April 2004)

Electrorheological (ER) fluids placed between two barriers have the ability to change some of their physical properties like the apparent viscosity and modulus of elasticity when an external electrical field is applied. Early investigations of the sound transmission loss (STL) under DC voltage showed that a normal stress that develops in ER fluid in response to an electrical field has a significant influence on the magnitude of STL. The tangential (shear) stress had only a negligible effect on the STL. The aim of this study was to investigate the STL using a two-barrier system with ER fluid placed between them, and subjected to alternative voltage. The STL was investigated for various kinds of ER fluids in the presence of the variable alternative electric field density. The results showed that the STL had decreased with the increasing electric field density.

1. Introduction

Among smart materials, controllable fluids are materials that respond to an applied external field with a change in their rheological behavior. They generally are called “rheological fluids” or RF. Fluids or exact suspensions that respond to an applied external electric field are called “electrorheological fluids” (ERF). Those that respond to applied external magnetic field are called “magnetorheological fluids” or MRF. The response of the RF to an applied field is manifested when the fluids are sheared by the force, creating a yield stress that is more or less proportional to the magnitude of the applied field. Their fluidity is manifested by change in apparent viscosity.

Generally, RFs are non-colloidal suspensions of polarizable particles having a size on the order of a few microns. MRF should not be confused with colloidal ferrofluids, in which the particles are about 1×10^3 times smaller than those found in typical MRFs.

The ER effect is also called the Winslow effect, after the person who first described this phenomenon in 1949. The discovery and development of MRF can be credited to Jacob Rabinow at the US National Bureau of Standards in 1940.

Generally, ERFs consist of solid particles which is a solid phase dispersed in insulating liquid or liquid-phase. Under the influence of electric field particles, the solid phase tends to form chains and columns along the direction of an applied electric field. This results in enhanced shear stress and such fluid exhibits increased resistance to flow. Apparent viscosity increases as well as elastic modulus. The increased stiffness is observed. For those reasons, the transition has been described as liquid-solid [10–21].

Both ERFs and MRFs are semi-active, in the sense that one can only resist flow on an applied shear force, not generate them. Generally, MRFs and ERFs are complementary rather than competitive with each offering specific advantages or disadvantages that make them suitable for different applications. Interest in these controllable fluids derives from their ability to provide simple, quiet, rapid response and interfaces between electronic controls and mechanical systems. It has long been recognized that controllable fluids have the potential to radically change the way electromechanical devices are designed and operated.

Drivers are frequently exposed to shock when their vehicle encounters irregularities on the road. Often the seat suspension does not have sufficient displacement (runs out of travel), and drivers experience the phenomenon known as “topping” and “bottoming”.

It is well known that exposure to shock increases the risk of spinal injury and lower back pain for occupational drivers. Extremely high levels of shock, such as those encountered in a car accident, can cause compressive fracture of the spine, while chronic exposure to lower-levels can lead to disc degeneration and lower back pain. Drivers that experience frequent “bottoming” and “topping” can also lose temporary control of the vehicle. The common design of the driver’s seat utilizes passive dampers to isolate the driver from vibration and in the case of heavy equipment, the seat is equipped with an air-ride suspension. This design isolates the driver from the average level of vibration in 3 to 10 Hz range. However, the problem of “bottoming” and “topping” exists because the damper is too “soft”. Many designs provide elastomer snubbers to absorb impact energy, but they generally do not provide adequate protection for the driver.

In 1998, Lord Corporation introduced the “Motion Master Ridge Management System” to the truck industry. This system consists of a controllable damper (controllable cylinder-piston shock absorbers) filled with MRFs and sensors that measure the position of the seat suspension. A controller with programmed algorithm adjusts the damping force in response to change in seat position. Damping force can be adjusted up to 500 times per second. The Lord Corporation claims that the percent of reduction in Vibration Dose Value (VDV) and the shock defined by maximum acceleration transmitted to a 200-pound driver by up to 40% and 49%, respectively.

Currently, the automotive industry presents applications of MRF in the Cadillac Seville STS and the 2004 Cadillac SRX and XLR roadster models. The 2003 Chevrolet Corvette also utilizes MRFs in its suspension system. Ford focuses research towards the use of MRFs in clutches to control the transfer of torque and to apply MRF dampers

in steering columns to better dissipate energy in front or rear end collisions. Active and semi-active MRF engine mounts may further reduce vibration and quiet noise before it enters the interior of a vehicle.

The Cadillac model SRX luxury car introduced, under the name of “Magnetic Ride Control”, controlled MRF-type dampers independently at each wheel. Cadillac claims that this is the world’s fastest reacting suspension system with a virtually infinite number of adjustments. The response of the system gives opportunity to read every inch of the road at a speed of 60 mph and adjust resistance to movement of the MRF damper to the specific surface of the pavement. This semi-active suspension system enables fast response for better performance, virtually silent operation, and the elimination of electromechanical valves. Benefits also include a $\sim 40\%$ reduction in mechanical parts associated with suspension systems. The system’s electronic control unit sends electrical current to electromagnetic coils housed in the dampers filled with MRFs. The current alters the MRF yield stress and, therefore, damping resistance. The flow of MRFs in the damper is also controlled. The magnitude of damping levels can be adjusted with a frequency up to 1 KHz with no lag. In 2000, Cadillac revealed the Imaq model, where “Magne Ride” is linked to the “Stabili Track” system and provides a very smooth ride, a high level of vehicle stability, control, and safety.

The Smart Technology Ltd. is located in Birmingham, England and is developing ERF-based suspension damping systems with plans to initially target European car manufacturers. They claim that ERFs present a lack of hysteresis in comparison to MRFs. Because MRFs are ferromagnetic, residual particle interface can occur, resulting in tiny oscillations, which slip past MRF shock-absorption systems because they are below the forces necessary to activate the material’s damping effect. ERFs do not exhibit the same residual yield stress as MRFs.

The forklift industry applied MRFs in the area of steer-by-wire, in which no mechanical connection exists between the steering wheel and the drive wheels. This technology is applied to brake-by-wire, clutch-by-wire, and shift-by-wire systems. The traditional mechanical and pneumatic or hydraulic components are replaced with electric wire connections, enabling manufacturers to simplify design and reduce vehicle weight.

Japan was the first country to implement MRF damping systems to stabilize buildings against earthquakes. The best-known building is the Museum of Emerging Science and Engineering in Tokyo. A computerized system senses the motion of the ground during an earthquake and sends current to magnetic coils in the dampers. The dampers provide the necessary resistance to the displacing forces [14].

China utilizes MRF dampers to stabilize motion of Dong Ting Lake Bridge in high winds. Dampers are applied to the diagonal cables on which the bridge’s structure is attached.

QED Technologies, based in Rochester, New York, utilizes polishing material based on MRFs. The rate of material removed is proportional to the magnetic field applied. This technology gives excellent results in the final polishing of precision optical lenses.

Lord Corporation USA developed MRF dampers for washing machines, effectively lowering the level of the machines’ level of vibration and emission of noise.

Other applications are related to military equipment, such as an MRF system for damping barrel recoil and dampers for helicopter blades.

Biedermann Motech GmbH, Schwenningen, Germany, introduced a Smart Magnetix advanced prosthetic knee in 2000, developed in collaboration with Lord Corporation. This “smart” prosthetic knee system, based on a controllable MRF damper, was commercially accepted by the orthopedics and prosthetic market. The classical design of artificial knees that features pneumatic or hydraulic cylinder-piston damper for momentum phase control cannot be adjusted in real-time to accommodate various gait conditions. The gait of the wearer of such a system is analyzed in a clinic and the damping characteristics of the classical damper are adjusted. The result of that adjustment/setting is very subjective in nature and average settings cannot be accurate in changing conditions during walking. Changes of surface conditions, temperature, and weight of the person’s shoe are not taken into account. Additionally, the various gait conditions cannot be adjusted in real-time. They must be manually changed to go from one mode to another.

The Smart Magnetix prosthetic knee comprises a thigh part that forms a socket for the leg stump, a knee joint, a lower leg assembly, and foot. The foot features a leaf spring to enable storage of some step energy that enables a springy step. The knee joint, in a form of complex hinges, also contains an important damper. The damper housing is linked to the shinbone-part of the prosthesis while the piston rod is attached to the knee joint. In the Smart Magnetix design, a controllable MRF damper is utilized. An electromagnet located inside the damper is controlled by an external electrical signal and provides the magnetic field that acts upon the MRF. A group of sensors are used to determine the instantaneous state of the knee-knee angle, swing velocity, axial force, and bending moment. A rotary position sensor at the knee pivot provides the knee angle position and velocity rate information. Strain gauge sensors above the shin attachment point provide axial force and bending moment signals. A microcontroller receives those signals and determines the electrical current needed to be applied to the MRF damper to allow for proper motion or locking of the artificial knee based on the instantaneous action being carried out by the user. Once calibrated to a specific person, the system automatically adapts in real-time to the user’s walking speed, stairs, slope of terrain, weight of the leg and changes in temperature. The system operates from a rechargeable battery. Physically, the damper is small. The body length is 90 mm and is 40 mm in diameter; the stroke is ± 15 mm. The power of about 5 watts is required to operate the damper at its nominal maximum design current of 1 amp. Although the damper contains about 35 cm^3 of MRF, the amount of fluid is activated in the piston orifices (magnetic valve) at any given instant is only about 0.43 cm^3 . It is possible to design an ERF valve that is normally closed and opens when power is applied. Using MRFs is generally much more efficient in redirecting the magnetic flux from the primary flow channel to a secondary, high-reluctance gap than attempting to directly cancel the permanent magnet. Since MR fluids have viscosity, there will always be an open-valve pressure drop, depending on flow rate. The lower the open-valve pressure drop, the larger the overall valve must be.

Smart Technology is developing an ERF-based Braille display tablet for the visually impaired. Current devices on the market allow users to either read or write. The proposed design by Smart Technology is an integrated ERF input-output interface that enables users to do both. A single line displays about 40 Braille characters. The full-size graphical array will feature 128×64 individual actuators that display either Braille characters or even simple graphics.

Bar-Cohen-Mavroidis are developing prosthetic devices for rehabilitation using MRFs, such as knee braces that resist the motion of the knee for rehabilitative training. A microprocessor controls the amount of force and a doctor can tailor the training program to specific patients. Another project is the On Demand Operational Exoskeleton (ODOE), a type of virtual reality suit to combat muscle atrophy in near-zero gravity. The concept involves mounting a robot on a robotic arm in space that performs external vehicle activities while the operator, seated inside wearing the ODOE, controls the robot's movements. Because ERFs mimic the rheology of biological tissues, Bar-Cohen also developed a training system for surgeons by having them operate on virtual patients using smart fluids to simulate the resistance of human flesh.

Electrorheological fluids (ERF) have a shear yield stress on an order of magnitude lower than MRF counterparts. The ERF-based damper would require, according to the "minimum active volume rule", about 40 cm^3 of the active fluid inside the piston's orifices at any given instant.

The current developments show that hybrid actuators can be implemented in many areas of engineering. Hybrid actuators would have one component with ERFs to resist external forces and electromagnetic actuators to generate new forces.

2. Mechanical characteristics of rheological fluids

2.1. Viscosity (η)

The dynamic viscosity η of rheological fluid depends on dynamic viscosity of the base liquid, the volume fraction of solid particles, the amount and type of additives used to control particle settling and the shear rate at which viscosity is measured. The water-based fluids have a higher particle volume fraction than the other oil-based fluids. The additives in the fluid cause the viscosity to increase rapidly when shear rate decreases. The apparent viscosity of the rheological fluid becomes lower when shear rate increases until it eventually reaches a steady state value. This phenomena is called "a shear thinning" character. For oil-based fluids, the apparent viscosity reaches a steady state value at a relatively low shear rate of perhaps a few hundred sec^{-1} . For the water-based fluids, the apparent viscosity starts higher at low shear rate and continues to drop over a much longer range of shear rate. In this case, an asymptotic, steady state value will not be reached until the shear rate increases up to several thousand or even ten thousand sec^{-1} . At these high rates, the water-based fluid will actually have lower apparent viscosity than the oil-based fluid.

2.2. Shear stress (τ)

The shear stress developed by an electrical field in ER fluids can be described using the Bingham model of plastics and this model is used most frequently [15, 16, 36].

$$\tau = \tau_y + \eta_{pl} p', \quad \tau \geq \tau_y, \quad (1)$$

where τ – shear stress, τ_y – static yield point shear stress, η_{pl} – plastic viscosity, p' – shear rate.

The Bingham model can also be represented as the bi-viscous model which couriers a “pre-yield” region where the ER suspension behaves as the Newtonian fluid.

It is represented as:

$$\tau = \begin{cases} \eta p' & |\tau| < \tau_1, \\ \tau_y + \eta_{pl} p' & |\tau| > \tau_1, \end{cases} \quad (2)$$

where η – viscosity of the pre-yield region, τ_1 – threshold value of shear stress distinguishing pre-yield and post-yield region.

That models (1), (2) show that, under shear stress, displacement will not occur until the yield stress has been overcome. Below the yield stress the ER suspension is solid like above this value it behaves as of liquid with very high viscosity. Most of results show shear stress in the range of several hundred N/m².

The Bingham model is valid for uniform, steady flow situations, where transient or “start up” effects are unimportant or neglected. It is not adequate for cases where transient behavior is important or when fluids are under dynamic loading, where rapid or impact stresses and damping must be considered.

2.3. Normal stress (σ)

The use of RF under comprehensive stress has been investigated since 1991 [27]. Initially they appear to act as Newtonian fluids, but the onset of Bingham plasticity follows abruptly when the applied field density reaches a certain point. This results in an increase in the hardness of the RF. The published data [34, 35] shows that the hardened suspension can withstand normal stress in excess of 1 GN/m².

2.4. Young's and bulk modulus of elasticity

The hardened suspension of RF fluid under electric field shows increase of Young's modulus of elasticity.

$$E_i = \frac{-d\sigma_i}{d\varepsilon_i}, \quad i = x, y, z, \quad (3)$$

σ_i – normal stress in x , y or z direction, ε_i – elongation in x , y or z direction.

It is known that E_i in RF shows strong dependence on direction of applied field. Young's Modulus of Elasticity is valid only in one degree of freedom systems (IDOF).

The bulk modulus of elasticity describes strength of hardened suspension of RF in volume, This is a three degree of freedom system (3DOF).

$$E_b = \frac{dp}{d\varepsilon_e}, \quad (4)$$

$$\varepsilon_e = \frac{dV}{V}, \quad (5)$$

where p – applied pressure, V – *initial* volume.

The value and changes of bulk modulus of elasticity of RF under applied filed have not been investigated. It is known, however, that the initial value of E_b for zero applied field is approximately equal to E_b of fluid phase in the RF.

Table 1. Representative controllable fluid properties.

Property	MR fluid	ER fluid
Max. yield stress	50–100 kPa	2–5 kPa
Max. field	~ 250 kA/m (limited by saturation)	~ 4 kV/mm (limited by breakdown)
Viscosity	0.1–1.0 Pa-s	0.1–1.0 Pa-s
Operable temp. range	–40 to +150°C (limited by carrier fluid)	+10 to +90°C (ionic, DC) –25 to +125°C (non-ionic, AC)
Stability	unaffected by most impurities	cannot tolerate impurities
Response time	< milliseconds	< milliseconds
Density	3–4 g/cm ³	1–2 g/cm ³
η_p/τ_y^2 (field)	10 ^{–10} to 10 ^{–11} s/Pa	10 ^{–7} to 10 ^{–8} s/Pa
Max. energy density	0.1 Joule/cm ³	0.001 Joule/cm ³
Power supply (typical)	2–25 V @ 1–2A (2–50 watts)	2–5 kV @ 1–10 mA (2–50 watts)
Ancillary materials	iron/steel	any conductive surface
Volume of RF necessary to operate	low	high

2.5. Valve Mode and Direct Shear Mode

Design of devices that use ER fluids can be classified as having either fixed poles (Valve Mode – “flow” or “no flow”) or relatively moveable poles (Direct Shear Mode – “motion” or “no motion”).

The Valve Mode is also recognized in literature as a “pressure driven flow mode” Examples include servo – valves, dampers and shock absorbers. Examples of Direct Shear Mode devices include clutches, brakes, chucking and locking devices.

A third mode of operation known as “squeeze-film mode” has also been used in low motion, high force applications.

The pressure drop developed in a design based on pressure driven flow mode is

$$\Delta p = \Delta p_{\eta} + \Delta p_{\tau}, \quad (6)$$

and

$$\Delta p = \frac{12\eta QL}{g^3 w} + \frac{e\tau_y L}{g}, \quad (7)$$

where L – active length, g – active thickness, w – active width, Q – intensity of flow, η – dynamic viscosity of liquid phase (no applied field), τ_y – shear yield stress developed in response to an applied field, e – factor,

$$e = 2 \quad \text{for} \quad \frac{\Delta p_{\tau}}{\Delta p_{\eta}} \leq 1, \quad (8)$$

$$e = 3 \quad \text{for} \quad \frac{\Delta p_{\tau}}{\Delta p_{\eta}} > 100. \quad (9)$$

The force developed in a direct-shear design is:

$$F = F_{\eta} + F_{\tau}, \quad (10)$$

$$F = \frac{\eta SA}{g} + \tau_y A, \quad (11)$$

where A – active shear area and $A = L^*w$, S – relative pole velocity.

2.6. Power required, stability yield stress and minimum active volume of typical commercial rheological fluids

(A) Power

Both ER and MR fluids devices in average applications have similar power requirements of about 50 W. The difference is in applied voltage and current requirement (see Table 1). ER fluid devices require high voltage 2–5 kV and low current 1–10 mA power supply, while MR fluid devices can be powered by low voltage 2–25 V and 1–2 A current power supply.

Required minimum power (in Watts) can be calculated from following semi-empirical equations.

$$P_{\text{MRF}_{\min}} = \frac{0.1 \cdot \text{MAV}}{\Delta t} \quad (12)$$

and

$$P_{\text{ERF}_{\min}} = \frac{0.001 \cdot \text{MAV}}{\Delta t}, \quad (13)$$

where Δt – desired switching time in seconds, MAV – minimum active volume.

(B) Stability

The MR fluid is resistant to the some extend to contaminants and/or impurities. The ER fluid is highly sensitive to any contaminants and/or impurities including water condensation from atmosphere. Currently ERF last only a few months in heavy-duty applications. The MR fluid is highly prone to setting of the solid phase in the suspension.

The physical properties of all RF are additionally strongly temperature dependant.

(C) Yield stress

Magneto-rheological fluids have a shear yield stress on order of magnitude greater than Electro-rheological counterparts.

$$\tau_{Y_{\text{MRF}}} = 50 \div 100 \text{ kPa}, \quad (14)$$

$$\tau_{Y_{\text{ERF}}} = 2 \div 5 \text{ kPa}. \quad (15)$$

(D) Minimum Active Volume (MAV)

The yield shear stress of the RF indicate that for comparable mechanical performance volume of the active fluid needed in ER design is about two orders of magnitude greater than that of MR design

$$\text{MAV}_{\text{MRF}} \cong \alpha P \left(\frac{F_{\text{ON}}}{F_{\text{OFF}}} \right) \cdot 10^{-4}, \quad (16)$$

$$\text{MAV}_{\text{ERF}} \cong \alpha P \left(\frac{F_{\text{ON}}}{F_{\text{OFF}}} \right) \cdot 10^{-2}, \quad (17)$$

where for rotary application (shear) $\alpha = 1$, for linear application (valve) $\alpha = 2$, P – required power in Watts, F_{ON} – minimum “on-state” force in N, F_{OFF} – minimum “off-state” force in N.

3. ER fluids and the measurements

The liquids that have been employed in the measurements were suspensions of zeolite particle (20% and 30% of weight, respectively) in a transformer oil. Additional investigations were conducted on the modified commercial liquid VersiFloTM ER-201 from the Lord Corporation [33]. The modification was done by adding some transformer oil to ER-201 so the final product was 80% suspension (weight) of ER-201 in the transformer oil. The reason was that initially the ER-201 was too dense and was difficult to mix after the solid particles in suspension sedimented in the electrode system. In that case the results of STL measurements were very inconsistent.

All experiments were conducted at the temperature of 20°C (293 K). Humidity in the laboratory where the measurements were done was kept constant, within the range of 50–60%.

Instead of using a large reverberation room and an anechoic chamber or two reverberant rooms, it is possible to work with two chambers. As a sound source system in the primary chamber, a sine generator along with an amplifier and a speaker are used. The secondary or receiving chamber is placed behind the sample. The system is presented in Fig. 1. The sample that is placed between two standing wave tubes (which are utilized chambers) is a system of two electrodes with an ER fluid between the electrodes powered by the high voltage AC power supply. Two electrode systems are designed: in the first one the direction of the electric field and the sound wave propagation are perpendicular. In the second the direction of the electric field and the sound wave propagation are parallel.

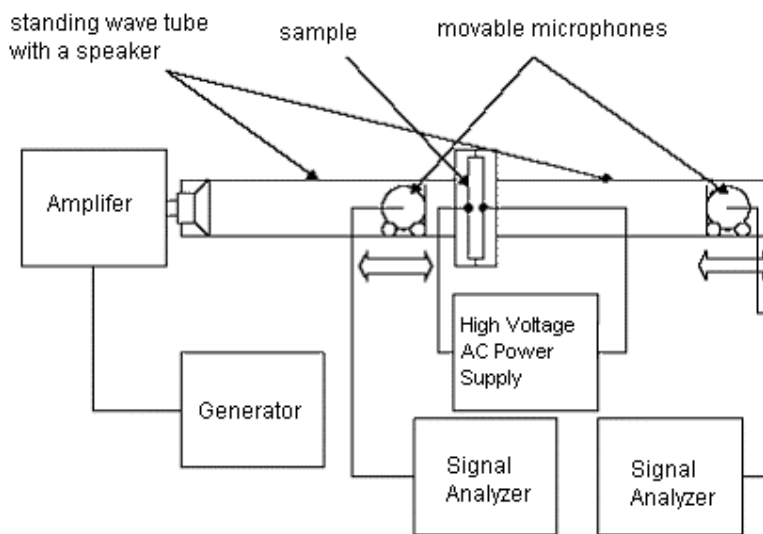


Fig. 1. Proposed measurement system.

Signal analyzers allow for examination of two signals: one of them is the source sound, the second is the sound after it passes through the system of electrodes. Both signals are analyzed for approximately 1/3 of the octave of frequency 100 and 800 Hz.

4. Results

(A) Results of the STL measurements for the AC electric field parallel to the direction of the sound wave

This portion of experiments was conducted using the parallel plate configuration of electrodes (Fig. 2). Figure 3 presents the sound transmission loss for 30% suspension of zeolite in transformer oil; the STL curves are shown for the frequencies of 100, 400, 800, and 1200 Hz and for the various levels of the electric field density.

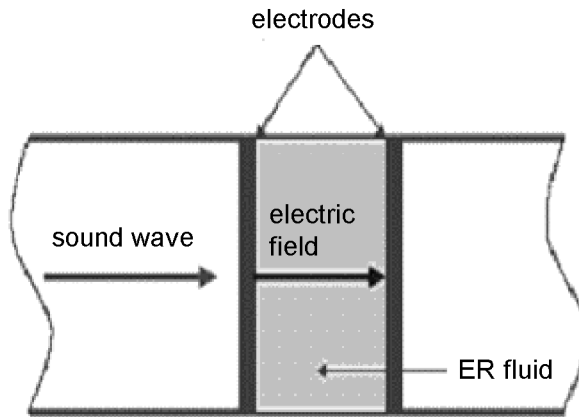


Fig. 2. Measurements of the STL with the electric field parallel to the wave direction.

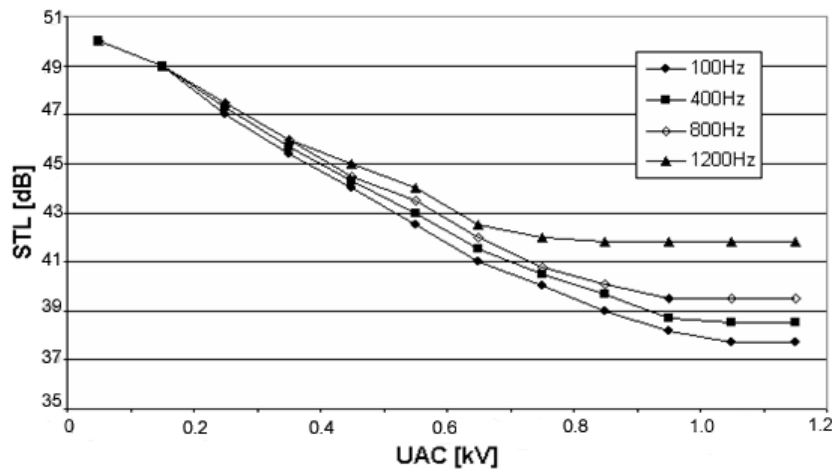


Fig. 3. Sound transmission Loss for 30% zeolite in the transformer oil. The electric AC 100, 400, 800 and 1200 Hz field parallel to the sound wave.

It can be noticed that the increase in the electric field density, results in the lowering of the sound transmission loss values. Application of the electric field allows for more of the sound to go through the whole structure and seems to be of a greater value for the low frequencies 100–250 Hz. The power of the transmitted sound increased four times where the STL drop was the biggest (11.8 dB drop for 30% zeolite suspension).

(B) Results of the STL measurements for the AC electric field perpendicular to the direction of the sound wave

For this part of the experiments the electrode system shown in Fig. 4 was used. The results are presented in Fig. 5. The STL drop for this configuration of electrodes was

not very significant, though one should notice that the active surface of electrodes was very small. After application of the highest electric field density level of 1 [kV/mm] the biggest STL drop for the ER201 suspension was 3 [dB].

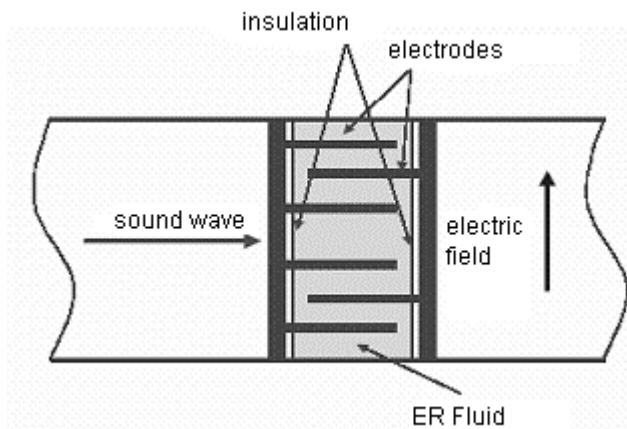


Fig. 4. Measurements of the STL with the electric field perpendicular to the wave direction.

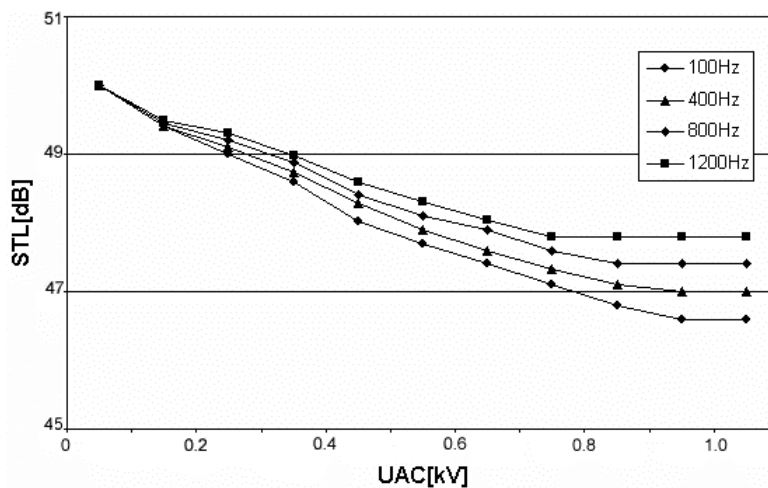


Fig. 5. Sound transmission loss for 30% zeolite in the transformer oil. The electric AC 100, 400, 800 and 1200 Hz field perpendicular to the sound wave.

5. Recapitulation

Characteristics given in Figs. 3 and 5 indicate that the density of the electric field does affect the STL of ER suspensions. It was observed that with the increase of the voltage between electrodes the transmission loss was decreasing for all the ER fluids at all the measurements frequencies. The most significant STL drop was observed for the

frequency range from 100 to 250 Hz. The liquid that seemed to show the biggest STL drops was 30% suspension of zeolite in the transformer oil. There are many possible explanations for the effect; one might make use of the mechanical coupling between electrodes via the ER liquid structure formed under influence of the electric field, another one can consider the electric forces interactions in ER suspension.

For the electric field perpendicular to the direction of the sound wave the graphs of STL vs. frequency (Fig. 5) do not show a significant STL change with an electric field increase. The active electrode area was very small in this particular case and that could be a possible explanation for the small STL drop. Another reason is that the shear stresses that ER fluids are able to withstand are 10–100 times smaller than corresponding compressive stresses. Although not very discernable, this STL drop effect was present and occurred for the entire measurement frequency range and for all three investigated suspensions. Again, as in the case of flat, plain electrodes configuration, the biggest drop in the STL values was registered for the 30% zeolite suspension.

The maximum transmission loss is:

$$\text{STL} = \text{STL}_{\max} \sin(n \cdot 180^\circ)$$

and was observed for:

$$U_{AC} = -U_{AC\max} \sin(n \cdot 180^\circ),$$

where $n = 0, \pm 1, \pm 2, \pm 3, \dots$,

The relationship between acoustical pressure on the surface of the barrier and applied AC voltage to the barrier to achieve required sound transmission loss is:

$$U_{AC} = U_{AC\max} \sin(n \cdot 180^\circ)$$

and

$$p = p_{\max} \cos(n \cdot 180^\circ)$$

where:

$$n = 0, \pm 1, \pm 2, \pm 3 \dots$$

There is also a quadratic relationship between STL and applied voltage.

6. Conclusions

- The sound transmission loss of ER suspensions can be controlled by the external DC or AC electric field. The STL of those ER liquids decreased with the increase of the electric field density applied. For a flat-parallel system, where the electric field was parallel to the direction of the incident sound wave (Figs. 2 and 3), the sound transmission loss drop was up to 12 dB for the highest (1 kV/mm) electric field density applied.
- The observed STL drop values were higher for the lower frequency range of the measurement band 100–250 Hz for all the suspensions and transformer oil as a liquid phase.

- The STL drop was also observed in the electrode system where the electric field was perpendicular to the direction of the sound wave – the values of that drop were not high (maximum of 3.3 dB was observed at the frequency of 100 Hz for the 30% suspension of zeolite in the transformer oil).
- Potential applications are semi-active STL controllers, especially in the low frequency range, active noise control devices, etc.

References

- [1] SZARY M. L., *Experimental study of sound transmission loss in electrorheological fluids under DC voltage*, Archives of Acoustics, **27**, 3 (2002).
- [2] SZARY M. L., *Sound transmission loss through two barrier systems with electrorheological liquid*, Tenth International Congress on Sound and Vibration, 7–10 July Stockholm 2003.
- [3] SZARY M. L., *Experimental study on sound transmission loss in electrorheological liquid under stress developed by DC voltage*, International Congress and Exposition on Noise Control Engineering, 19–21 August, Detroit, Michigan 2002.
- [4] SZARY M. L., NORAS M., *Experimental study of sound transmission loss in electrorheological fluids*, Proceedings at Conference on Noise Control, 401–408, September, 24–26, 2001, Kielce, Poland.
- [5] JOLLY M. R., BENDER J. W., MATHERS R. T., *Indirect measurements of microstructure development in magnetorheological fluids*, Int. J. of Modern Physics B, **13**, 14–16, 2036 (1999).
- [6] NAKANO M., YAMAMOTO H., JOLLY M. R., *Dynamic viscoelasticity of a magnetorheological fluid in oscillatory slit flow*, Int. J. Modern Physics B, **13**, 14–16, 2068 (1999).
- [7] LY H. V., REITICH F., JOLLY M. R., BANKS H. T., ITO K., *Simulations of particle dynamics for magnetorheological fluids*, J. Computational Physics, 155, 160–177 (1999).
- [8] JOLLY M. R., BENDER J. W., CARLSON J. D., *Properties and applications of commercial magnetorheological fluids*, SPIE 5-th Annual Int. Symposium on Smart Structures and Materials, San Diego, CA, March 15, 1998.
- [9] CARLSON J. D., CATANZARITE D. N., ST. CLAIR K. A., *Commercial magneto-rheological fluid devices*, Proceedings 5th Int. Conf. on ER Fluids, MR Suspensions and Associated Technology, W. BULLOUGH [Ed.], World Scientific, Singapore, 20–28, 1996.
- [10] KOROBKO E. V., SHULMAN Z. P., VORONOVICH G. V., *Electrorheological damping in precision systems*, Proceedings Of SPIE, 3041, 868–873, Smart Structures and Materials, 3–6 March 1997, San Diego, CA., Bellingham, Wash., SPIE, 1997.
- [11] PEEL D. J., STANWAY R., BULLOUGH W. A., *The ER long-stroke damper: experimental verification of mathematical models*, Rheology and Fluid Mechanics of Nonlinear Materials, FED-243/MD-78, 249–259, ASME, 1997.
- [12] CHOI S., PARK Y., CHEUNG C., *Active vibration control of intelligent composite laminate structures incorporating an electro-rheological fluid*, Journal of Intelligent Materials Systems and Structures, **7**, 411–419 (1996).
- [13] GAVIN H. P., HANSON R. D., *Electrorheological devices with annular electrodes*, Proceedings of 10-th Conference ASCE, Boulder, CO., May 21–24, 2, 1231–1234, ASCE, New York 1995.

- [14] DYKE S. J., SPENCER B. J., Jr., SAIN M. K., CARLSON J. D., *Seismic response reduction using magnetorheological dampers*, Proceedings of the IFAC World Congress, San Francisco, Ca., June 30-July 5, 1996.
- [15] BLOCK H., KELLY J. P., *Electro-rheology*, Journal Of Physics D, Applied Physics, **21**, 12, 1661–1667 (1988).
- [16] JORDAN T. C., SHAW M. T., *Electrorheology*, IEEE Transactions On Electrical Insulation, **24**, 5, 849–878 (1989).
- [17] KLASS D. L., MARTINEK T. W., *Electroviscous fluids II. Electrical properties*, Journal of Applied Physics, **38**, 1, 75–80 (1967).
- [18] SHIANG A. H., COULTER J. P., *A Comparative study of AC and DC electrorheological material based adaptive structures in small amplitude vibration*, Journal of Intelligent Materials Systems And Structures, **7**, 455–469 (1996).
- [19] KUDALLUR S., CONNERS G. H., BUFFINTON K. W., *Electrorheological damper for precision applications*, Developments in Electrorheological Flows, ASME, FED-235/MD-71, 21–27 (1995).
- [20] CONRAD H., CHEN Y., *Electrical properties and the strength of electrorheological (ER) fluids*, Progress in Electrorheology, HAVELKA K. O., FILISKO F. E. [Eds], 55–85, Plenum Press, New York 1995.
- [21] RADCLIFFE C. J., LLOYD J. R., ANDERSLAND R. M., HARGROVE J. B., *State feedback control of electrorheological fluids*, presented at ASME International. Congress & Exhibition, November 17–22, Atlanta, GA, 1996.
- [22] LEITMANN G., *Semi-active control for vibration suppression in a system subjected to unknown disturbances*, Journal of Circuits, Systems And Computers, **4**, 4, 379–393 (1994).
- [23] RIBAKOV Y., GLUCK J., *Active control of mdof structures with supplemental electrorheological fluid dampers*, Earthquake Engineering & Structural Dynamics, **28**, 143–156 (1999).
- [24] MAEMORI K., SAJTO T., *A new type of hydraulic shock absorber using electrorheological fluid*, JSME International Journal, Series C, **41**, 1, 156–163 (1998).
- [25] LEITMANN G., *Semiactive control for vibration attenuation*, Journal of Intelligent Materials Systems and Structures, **5**, 841–846 (1994).
- [26] YALCINTAS M., COULTER J. P., *Electrorheological material based non-homogeneous adaptive beams*, Smart Materials & Structures, **7**, 128–143 (1998).
- [27] KLINGENBERG D. J., DIERKING D., ZUKOSKI C. F., *Stress-transfer mechanisms in electrorheological suspensions*, Journal of Chemical Society Faraday Transactions, **87**, 3, 425–430 (1991).
- [28] KOHL J. G., TICHY J. A., *Expressions for coefficients of electrorheological fluid dampers*, Lubrication Science, **10**, 2, 135–143 (1998).
- [29] PARTHASARATHY M., KLINGENBERG D. J., *Large amplitude oscillatory shear of ER suspensions*, Journal of Non-Newtonian Fluid Mechanics, **81**, 83–104 (1999).
- [30] Laboratory Measurement of the Airborne Sound Barrier Performance of Automotive Materials and Assemblies, SAE J1400”, May 1990.
- [31] NORAS M., *Sound transmission loss control using electrorheological fluids*, Ph.D. thesis, Southern Illinois University, December 1999.
- [32] BERANEK L. L., VER I. L., *Noise and Vibration Control Engineering: Principles and Applications*, Wiley, New York 1992.

- [33] VersaFlo™ Fluids Product Information: Lord® Corporation, Form# P101-ER201A.
- [34] MONKMAN G. J., *The electrorheological effect under compressive stress*, Journal of Physics D: Applied Physics, **28**, 588–593 (1995).
- [35] DAVIS L. C., GINDER J. M., *Electrostatic forces in electrorheological fluids*, Progress in Electrorheology, HAVELKA K. O., FILISKO F. E., Plenum Press 107–114, New York 1995.
- [36] CONRAD H., SPRECHER A. F., *Characteristics and mechanisms of electrorheological fluids*, Journal of Statistical Physics, **64**, 1073–1091 (1991).